The Synthesis and Application of the Bulkiest Imidodiphosphorimidate Brønsted Acid Catalyst

Junshan Lai and Jolene P. Reid*

Department of Chemistry, University of British Columbia, Vancouver, British Columbia V6T 1Z1, Canada

ABSTRACT: The development of BINOL-derived Brønsted acid catalysts has been profoundly guided by rational design, with carefully implemented structural changes leading to unique generations of catalysts with enhanced reaction capabilities. This approach to catalyst optimization has promoted the integration of knowledge gathered in optimizing prior eras of Brønsted acids and ultimately, the molecular features that have contributed to the success of previous designs are preserved. Of these, the large substituents at the 3 and 3' positions of the BINOL backbone are the most critical with almost every newly developed structure possessing this feature. However, imidodiphosphorimidate (IDPi) catalysts are not synthetically well-suited to contain the same sterically bulky groups associated with the high selectivity imparted by previously implemented catalyst structures. Herein, we have leveraged the moderate size (as compared to TRIP and 9-anthryl) but high applicability of the 9-phenanthryl substituent to synthesize an extremely sterically demanding IDPi. Using computed descriptors, we survey the catalyst properties of known structures to demonstrate this catalyst to be both unique and to the best of our knowledge, the bulkiest IDPi yet synthesized. The applicability of the catalyst was evaluated in the construction of stereochemically dense spirocycles generated via an asymmetric Prins-semipinacol reaction sequence. Transition state calculations were deployed to interrogate the origins of the superior enantioselectivity and these demonstrate the mechanistic hallmarks of the 9-phenanthryl substituent can be generalized to a genuinely different class of Brønsted acid catalyst.

The structure of chiral organocatalysts continues to evolve with each notable design gaining enhanced function over enantioselective bond construction.[1-2] Asymmetric Brønsted acid catalysis exemplifies this where iterative changes to the catalyst structure has enabled marked increases in selectivity and reactivity for a diverse set of organic transformations.[3-5] Indeed, these efforts have led to generations of rational catalyst designs that have developed from simple modifications of the catalyst substituents[6] to the introduction of strongly acidic dimeric catalyst structures (Figure 1).[7] Despite this significant progression in structure, new Brønsted acid catalysts typically retain the key molecular features that have led to a good performance with older designs. For example, N-triflyl phosphoramide catalysts were introduced to overcome the reactivity barriers associated with weakly basic carbonyl substrates but contain the same sterically bulky groups associated with the high selectivity imparted by BINOL-derived phosphoric acids.[8] Likewise, List's imidodiphosphates (IDP) enable highly enantioselective transformations of difficult substrates through the strict conformational confinement generated by the two binaphthol units and constrained by the large substituents at the 3 and 3' positions. Recent modifications to this scaffold has demonstrated the replacement of the catalyst oxygens with two N-triflyl groups leads to the highly acidic imidodiphosphorimidate (IDPi) catalysts.[9] However, IDPis have not yet benefitted from the knowledge gathered in optimizing previous eras of Brønsted acids. Accordingly, the substituents at the 3,3' positions are usually distinctive with well performing catalysts showing a large structural diversity (Figure 1).

Recently, our group has quantified the applicability of BINOL-derived chiral phosphoric acids using unsupervised

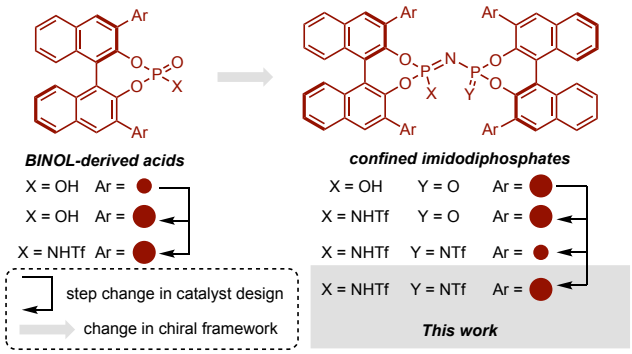

Figure 1. The evolution of Brønsted acid catalysts for enantioselective bond construction.

machine learning and the results of this computation showed certain 3,3' substituents are able to provide broad spectrum success.[10] Of these the most general structures possess either very large alkyl groups at the 2, 4 and 6 positions of the aromatic ring or contain extended π-systems. In many cases, catalysts bearing these large substituents are more adaptative to changes in reactant structure because enantioinduction does not rely on a single set of noncovalent interactions. For example, 9-phenanthryl derived catalyst structures can impart high levels of enantioselectivity by engaging in attractive or repulsive noncovalent contacts. In other cases, like TRIP, robust steric interactions are established and these do not change significantly nature when the structure of the reaction component is altered.

Considering this and the transferability of structural elements between distinct eras of Brønsted acid catalysts designs

we question if incorporating these groups can lead to well performing IDPi catalysts? To our knowledge, the effect of including such groups at the 3,3' positions has not been assessed, although this is largely because the chiral framework tends not to be synthetically well-suited to containing functionality that places additional steric bulk proximal to the phosphorous atom. The synthesis of these catalysts are challenging usually relying on a dimerization step which is strongly influenced by the steric properties of the 3,3'-substituents, if these are too big unsatisfactory yields are obtained or the reaction may fail to proceed altogether. In this context, we have taken advantage of the moderate size (as compared to TRIP and 9-anthryl) but high generality of the 9-phenanthryl substituent to synthesize a new IDPi that can facilitate a broad set of asymmetric Prins-semipinacol reactions to afford spircocycles in high levels of enantioselectivity.

Results and Discussion.

Trends and Molecular Descriptors. The structure of the substituents at the 3,3′ positions of the BINOL backbone have a considerable effect on the stereochemical outcome of many reactions, and, usually, large steric bulk is required for high enantioselectivity.[11-13] On this basis, we questioned what is the largest substituent that can be incorporated into the IDPi catalyst framework? To answer this question, we considered the size of 3,3' aromatic groups common to many Brønsted acids using two different measures of steric requirements (i) rotation barrier for a phenyl group, and (ii) A Remote Environment Angle: AREA(θ), a measure of space less close to the catalyst site.[11] At this initial stage of the study we are only concerned about the steric features exhibited by a portion of the IDPi catalyst such that these values do not need to be obtained from the whole molecule structure. Indeed, rotational barriers for a phenyl group are derived from the energy required for rotation around the central C–C bond. Because the interaction between the R groups and the hydrogens on the opposing aryl ring are responsible for the destabilization of the eclipsed conformation this descriptor can only account for nearby sterics. In contrast, the angle measurement AREA(θ), is sensitive to increases in the steric demands remote from the aromatic ring with substituents that crowd access to the phosphorus resulting in smaller values. To estimate if the incorporation of certain substituents could lead to a structure that would be both well performing and synthetically tractable, we next considered how these groups fit and operate within existing catalyst space. Visual inspection of reported IDPi catalysts, shows that 3,3' substituents only display a large structural variation in the remote positions of the aromatic ring. Therefore, the impact of introducing steric demands at positions close to the phosphorous is less clear, however, it is expected to lead to highly reactive and selective catalysts based on the information gathered from structurally familiar catalyst types. Key data is summarized in Figure 2B and these results indicate that the 9-phenanthryl group, bears steric demands similar to known IDPi structures. For example, the structural descriptors show that the proximal steric effect exerted by 9-phenanthryl will be similar to that of the 1-naphthyl substituent while the remote steric bulk is measured to be comparable to the 2-naphthyl group. This may be surprising and it is possible that the perceived significantly larger size of a 9-phenanthryl substituent has inhibited the investigation of these catalysts thus far. Intriguingly, this comparison also suggests that installing a 9-phenanthryl substituent upon the IDPi framework could allow access to the bulkiest catalyst structure yet prepared.

Motivated by the structural uniqueness afforded by this catalyst we attempted to synthesize the novel IDPi bearing a 9-phenanthryl group. The List group has reported several ways that enable access to this catalyst motif with the most common approach involving dimerization of the 3,3'-substituted BINOL-derivatives in the presence of an ammonia surrogate.[14] This factor, combined with the observation that particular IDPis containing substituents with similar steric features can be accessed in this manner, prompted us to explore the reactivity of the requisite 3,3'-substituted BINOL-derivative. Using this procedure we synthesized IDPi **2a**, obtaining 59% yield after 7 days (Figure 2C). This result is comparable to the synthesis of other IDPis which typically require prolonged reaction times of 3–4

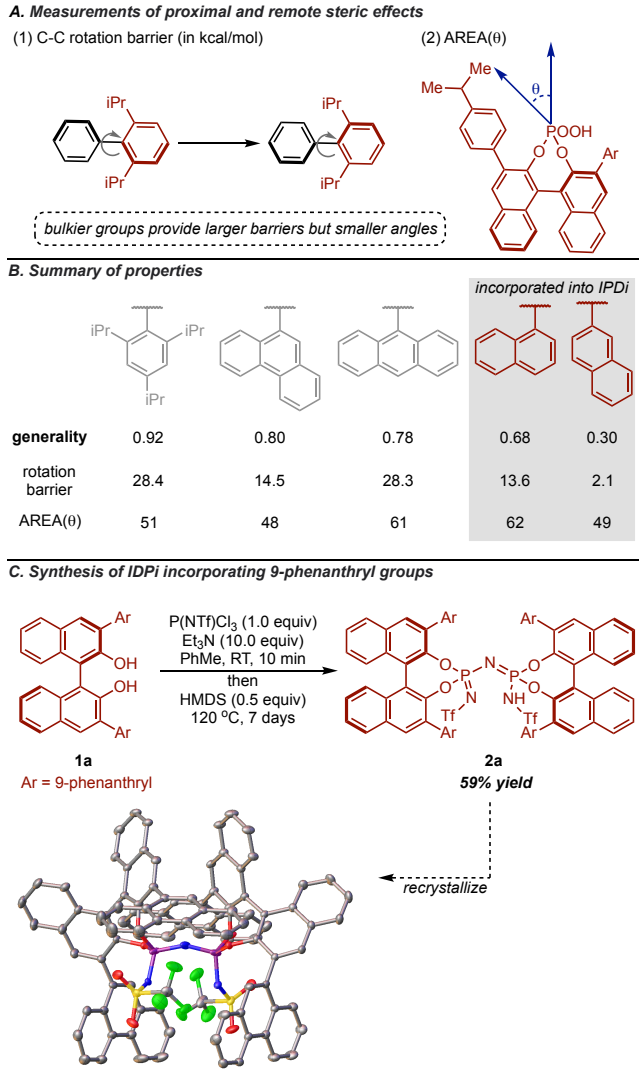

Figure 2. (A) Catalyst parameters evaluated in this study. Steric parameter (1) measures nearby bulk while (2) AREA(θ), accounts for steric effects distant from the phosphoric acid moiety. (B) Determining the synthetic feasibility of larger and more general catalyst groups. (C) Synthesis and structural analysis of an IDPi catalyst structure containing large 9-phenantryl groups.

days.[15] Attempted improvements to the catalyst synthesis focused on employing a recent strategy developed by the List group which have shown impressive outcomes in accessing sterically hindered catalysts.[16] Unfortunately, our efforts in applying this method to the synthesis of 2a did not yield desirable results. Structural crystallographic analyses of the imidodiphosphorimidate 2a reveals a highly confined chiral pocket created by the two BINOL backbones and constrained by the large 3 and 3' substituents (Figure 2C). The P–N–P bond angle (151.3°) was found to be significantly compressed relative to those structures bearing smaller groups previously reported by List (rotation barriers around 2.0 kcal mol^{-1} leads to angles of 160°–163°).[17] This distortion demonstrates that larger substituents force the structure to bend minimizing energetically repulsive contacts between the large 9-phenanthryl rings and the N-triflyl groups on the phosphorous.

Catalytic application. Having produced a Brønsted acid confined within an extremely sterically demanding chiral cavity, we examined the catalyst's aptitude to enforce high levels of enantiofacial discrimination for a continuous series of selective reactions. Because a single chiral catalyst must enable stereocontrol over discrete reaction events this approach to chiral molecule construction is much less common and to our knowledge, no examples have been reported with IDPis. These factors make sequential reactions an appealing assessment of the catalyst's ability to facilitate a difficult chemical transformation. In this context, we identified a Prins-semipinacol rearrangement as a stringent test that involves structurally unique reactive intermediates and bond forming steps to produce stereochemically dense spirocycles. In accord with previous studies,[18-20] we surmised that upon exposure of an aldehyde with a homoallylic alcohol an acid-catalyzed cyclocondensation would generate a carbocation and trigger a stereoselective skeletal rearrangement through the migration of the σ-bond. Central to the utility of this reaction sequence is the mechanistic requirement that any selectivity imparted in the semipinacol step is reinforced not eroded by the catalyst structure. Specifically, this would ensure high levels of diastereoselectivity for the overall process regardless of the stereochemistry set in the first key catalytic step. With this mechanistic print in mind, our investigation began by subjecting homoallylic alcohol **3** with aldehyde **4a** to the reaction conditions shown in Table 1. A catalyst evaluation showed popular IDPi's to provide insufficient enantioselectivities while our sterically bulky IDPi provided encouraging results. Switching the solvent to $CHCl_3$ and lowering the temperature allowed the spircocycle to obtained in 82% ee. Motivated by these results, further improvements to the enantioselectivity was achieved by decreasing the temperature from 0 °C to -20 °C but this tactic was limited to more reactive, electron rich aldehydes. Having developed optimal conditions for this new enantioselective Prins-semipinacol rearrangement sequence, we next examined the scope of the aldehyde component. As shown in Scheme 1, variations of the aryl component were generally well tolerated, although products bearing strongly electron withdrawing substituents were generated with lower enantioselectivities due to the higher temperature requirement. This lower reactivity with electron poor substrates is notable and consistent with a cationic charge developing in the rate determining step. Indeed, substrates with even greater electron withdrawing capabilities (e.g. CN and NO_2) failed to react at room temperature (see SI for more details). Exploration of styrenyl aldehydes showed less sensitivity to the electronic features of the aromatic ring having produced high levels of enantioselectivity across a diverse set substrates. To round out this aldehyde survey, we examined the use of heteroaromatics in the reaction relay. When progressing to this substrate class, we obtained some of the highest enantioselectivities observed thus far in any IDPi catalyzed reaction. Aldehydes bearing sterically demanding substituents also proved less selective and this may reflect the inability of our strictly confined acid to efficiently accommodate large substrates. The exquisite selectivity imparted by our confined catalyst is highlighted on comparing the diastereoselectivity created in the Semi-pinacol rearrangement under achiral and chiral conditions. More specifically, the data presented in Scheme 2 shows that the catalyst control matches the inherent stereoselectivity preference and were possible, enriches the selectivity. Further reaction insight was obtained from evaluating several designed homoallylic alcohols. The failure of these systems to react supports the crucial role of ring strain relief in driving the reaction forward.

Table 1. Optimization of the Prins-semipinacol reaction sequence.[a]

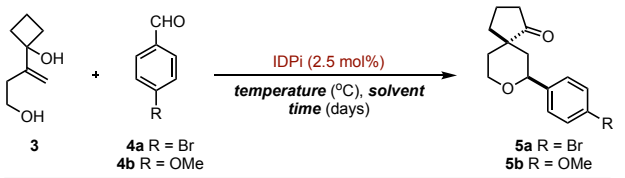

3 **4a** R = Br **4b** R = OMe **5a** R = Br **5b** R = OMe

entry	R	IDPi	*Temperature*	*Solvent*	*Time*	Yield[b] (%)	ee[c] (%)
1	Br	2a	RT	DCM	3	80	60
2	Br	2b	RT	DCM	3	79	30
3	Br	2c	RT	DCM	3	85	32
4	Br	2d	RT	DCM	3	82	14
5	Br	2a	RT	PhMe	3	72	66
6	Br	2a	RT	PhH	3	72	68
7	Br	2a	RT	DCE	3	80	46
8	Br	2a	RT	Et_2O	3	80	32
9	Br	2a	RT	$CHCl_3$	3	86	76
10[d]	Br	2a	0	$CHCl_3$	14	70	82
11	Br	2e	0	$CHCl_3$	14	72	60
12[d]	OMe	2a	0	$CHCl_3$	7	85	86
13[d]	OMe	2a	-20	$CHCl_3$	14	80	92

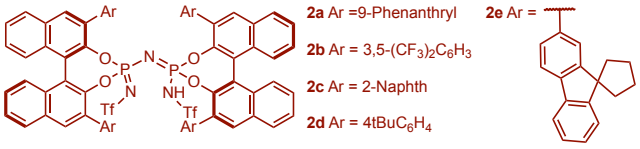

[a]Reactions were run with the following conditions: **3** (14.2 mg, 0.1 mmol, 1.0 eq), the aldehyde **4a** or **4b** (0.12 mmol, 1.2 eq) IDPi (2.5 mol%), solvent (0.5 mL). All reactions proceed with >99:1 dr. [b]Isolated yields given. [c]Enantioselectivities (ee) were measured by SFC. [d]Reactions run with 5 mol% catalyst loading. See the Supporting Information for further details.

Scheme 1. Various aldehyde substrates tested with the optimal conditions.[a]

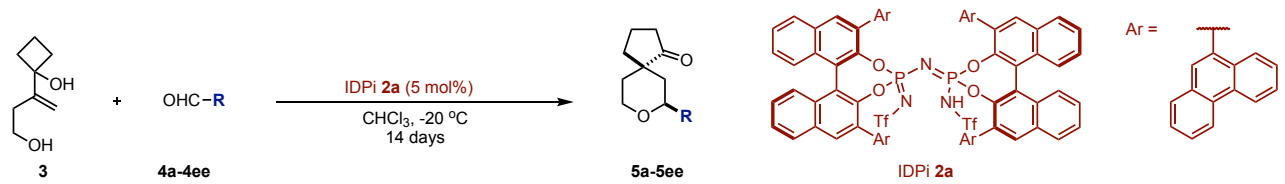

Aromatic and Styrenyl Aldehyde Substrates

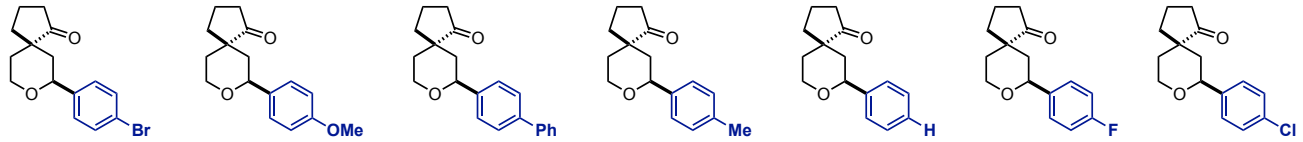

5a[b]: 70% yield, 82% ee | **5b**: 80% yield, 92% ee | **5c**: 69% yield, 85% ee | **5d**: 78% yield, 91% ee | **5e**: 72% yield, 85% ee | **5f**[b]: 75% yield, 82% ee | **5g**[b]: 67% yield, 83% ee

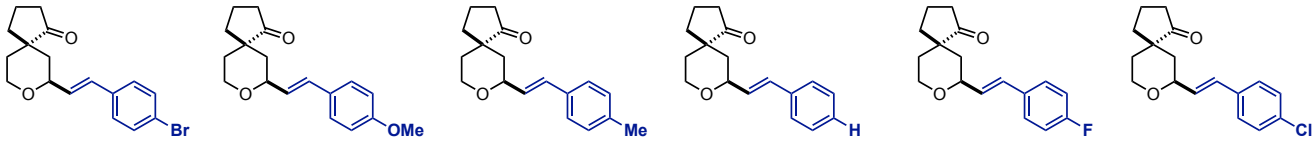

5h: 69% yield, 90% ee | **5i**[c]: 82% yield, 92% ee | **5j**[c]: 80% yield, 92% ee | **5k**[c]: 80% yield, 93% ee | **5l**: 79% yield, 92% ee | **5m**: 70% yield, 93% ee

Heteroaromatic Aldehyde Substrates

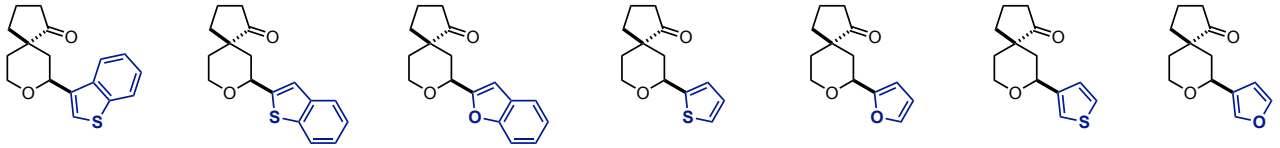

5n[b]: 75% yield, 90% ee | **5o**[b]: 66% yield, 93% ee | **5p**[b]: 65% yield, 96% ee | **5q**: 80% yield, 95% ee | **5r**: 75% yield, 97% ee | **5s**: 84% yield, 93% ee | **5t**: 68% yield, 92% ee

Aldehyde Substrates with Increased Steric Demands

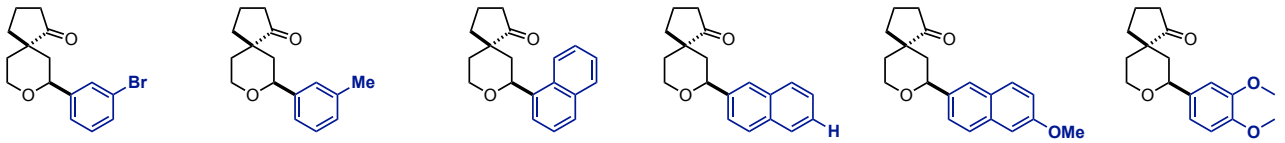

5u[d]: 68% yield, 70% ee[c] | **5v**: 72% yield, 84% ee | **5w**: 75% yield, 89% ee | **5x**: 68% yield, 82% ee | **5y**: 78% yield, 86% ee | **5z**: 88% yield, 50% ee

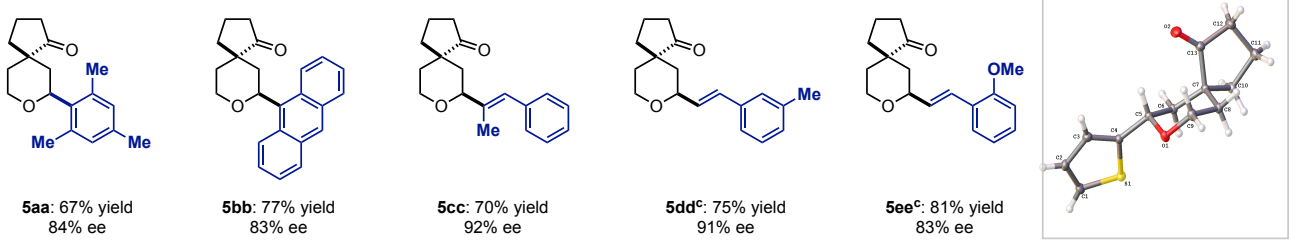

5aa: 67% yield, 84% ee | **5bb**: 77% yield, 83% ee | **5cc**: 70% yield, 92% ee | **5dd**[c]: 75% yield, 91% ee | **5ee**[c]: 81% yield, 83% ee

[a] Reaction conditions: **3** (14.2 mg, 0.1 mmol, 1.0 eq), the aldehyde **4a-4ee** (0.12 mmol, 1.2 eq) IDPi (5 mol%), $CHCl_3$ (0.5 mL). All reactions proceed with >99:1 dr. Isolated yields given. Enantioselectivities (ee) were measured by SFC. Absolute configurations confirmed by the X-ray crystallographic analysis after recrystallization of **5q**. The stereochemistry of the remainder of the entries is assigned by analogy. [b] Reactions were conducted at 0 °C for 14 days. [c] Reactions were conducted at -20 °C for 12 days. [d] Reactions were conducted at rt for 7 days.

To gain further insight into how the optimal IDPi imparts such high levels of enantioselectivity we computationally explored the Prins reaction event with ONIOM(ωB97XD/6-31G(d,p):UFF). This type of calculation allows larger systems like IDPi's to be explored efficiently without having the analysis limited to a few structures or a portion of the reactive

Scheme 2. Miscellaneous experiments

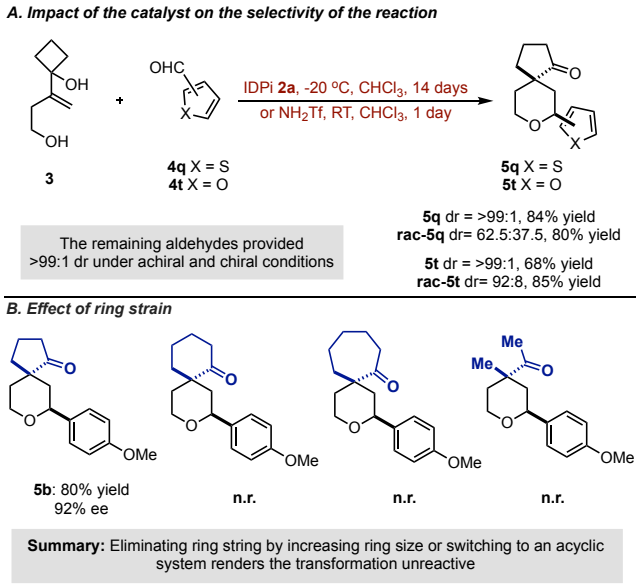

systems.[21] While these computational methods have been shown to give reliable results in various settings including those involving IDPi's - we were aware of the possibility of error. Accordingly, the lowest energy structures found from these calculations were submitted to full DFT geometry optimizations functionals to confirm the validity of our ONIOM results. The results of full DFT calculations can be found in the Supporting Information and show that interpretation of ONIOM structures and energies to be accurate. The calculations corroborate the observed high levels of enantioselectivity and sense of enantioinduction (Figure 3). We calculated the lowest energy transition state (TS) structure, **TS1-Si**, to bind to the catalyst through a single hydrogen bonding interaction only. The lower energy of a TS which lacks a second interaction from the catalyst to the oxonium hydrogen is unexpected, as double coordination modes are most likely. Comparable TS structures could be located in which the reactants establish two hydrogen bonding contacts, **TS2-Si**, and these would also lead to the experimentally observed enantiomer. In addition, we identified TS structures similar to **TS2-Si** which features the interaction from the catalyst to the oxonium proton, **TS2-Re**, but affords the competing product. Table 2 provides an overview of the key hydrogen bonding contacts established at the TS and these demonstrate the lowest energy structure features the weakest contacts. Further visual analysis reveals the most important difference between **TS(Si)** and **TS(Re)** is the absolute location and orientation of the 9-phenanthryl groups relative to the substrate. Visualization of **TS(Si)** shows that both structures position the substrate to maximize CH–π interactions with the aromatic groups. In contrast, **TS(Re)** forces the substrate to occupy the empty space between the large 9-phenantryl substituents. This is consistent with the primary determinants of enantioselectivity arising from these competing pathways being attractive noncovalent interactions with the 3,3' catalyst substituents and the substrate. The reasons for the energy differences between **TS(Si)** and **TS(Re)** were further investigated using distortion-interaction analysis (see SI).

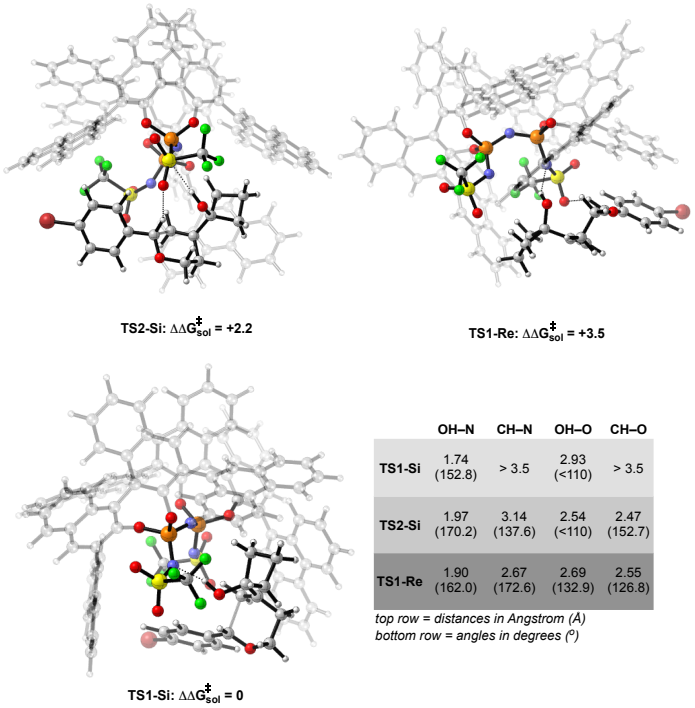

	OH–N	CH–N	OH–O	CH–O
TS1-Si	1.74 (152.8)	> 3.5	2.93 (<110)	> 3.5
TS2-Si	1.97 (170.2)	3.14 (137.6)	2.54 (<110)	2.47 (152.7)
TS1-Re	1.90 (162.0)	2.67 (172.6)	2.69 (132.9)	2.55 (126.8)

top row = distances in Angstrom (Å)
bottom row = angles in degrees (°)

Figure 3. Competing TS structures for the Prins reaction of homoallylic alcohol 3 with aldehyde 4a and catalyzed by IDPi. ONIOM(ωB97XD/6-31G(d,p):UFF). Solvent energies were derived from single point energies with IEFPCM ($CHCl_3$) model at the ωB97XD/6-311G(d,p) level. Grayed-out regions were treated with UFF, and the full-color regions were treated with ωB97XD /6-31G(d,p). All energies quoted in kcal mol^{-1}. Key hydrogen bonding features shown in the gray box.

Conclusion

We have achieved an enantioselective Prins-semipinacol reaction using an exceptionally bulky IDPi and investigated the unique capacity of this catalyst architecture to impart high levels of stereocontrol. Computational studies demonstrate attractive noncovalent interactions from aromatic groups on the catalyst and substrate determine the enantioselectivity, a distinctive feature of the 9-phenanthryl substituent in Brønsted acid catalysis. These findings suggest a probable general phenomenon, whereby various mechanistically unrelated transformations may be found to perform in the same manner when key catalyst groups are conserved between distinct eras of organocatalyst designs. Our ongoing and future studies are directed towards the generalization of substituent effects and leveraging this as a platform for catalyst design.

ASSOCIATED CONTENT

Supporting Information

Cartesian coordinates, energies of computed structures, experimental and X-ray crystal structure details (PDF).

AUTHOR INFORMATION

Corresponding Author

* jreid@chem.ubc.ca

ACKNOWLEDGMENT

Financial support to J.P.R. was provided by the University of British Columbia and the Natural Sciences and Engineering Research Council of Canada (NSERC). Computational resources were provided from Compute Canada and the Advanced Research Computing (ARC) center at the University of British Columbia. We thank the Huan group (UBC) for help with HRMS and Brian Patrick (UBC) for solving the crystal structure.

REFERENCES

[1] Doyle, A.G.; Jacobsen, E.N. Small-molecule H-bond donors in asymmetric catalysis. *Chem. Rev.* **2007**, *107*, 5713-5743.

[2] Han, B.; He, X.H.; Liu, Y.Q.; He, G.; Peng, C.; Li, J.L. Asymmetric organocatalysis: an enabling technology for medicinal chemistry. *Chem. Soc. Rev.* **2021**, *50*, 1522-1586.

[3] Kampen, D.; Reisinger, C. M.; List, B. Chiral Brønsted Acids for Asymmetric Organocatalysis. *Top. Curr. Chem.* **2010**, *291*, 395– 456

[4] Rueping, M.; Kuenkel, A.; Atodiresei, I. Chiral Brønsted acids in enantioselective carbonyl activations–activation modes and applications. *Chem. Soc. Rev.* **2011**, *40*, 4539-4549.

[5] Parmar, D.; Sugiono, E.; Raja, S.; Rueping, M. Complete field guide to asymmetric BINOL-phosphate derived Brønsted acid and metal catalysis: history and classification by mode of activation; Brønsted acidity, hydrogen bonding, ion pairing, and metal phosphates. *Chem. Rev.* **2014**, *114*, 9047-9153.

[6] Klussmann, M.; Ratjen, L.; Hoffmann, S.; Wakchaure, V.; Goddard, R.; List, B. Synthesis of TRIP and analysis of phosphate salt impurities. *Synlett* **2010**, *2010*, 2189-2192.

[7] Čorić, I.; List, B. Asymmetric spiroacetalization catalysed by confined Brønsted acids. *Nature* **2012**, *483*, 315-319.

[8] Nakashima, D.; Yamamoto, H. Design of chiral N-triflyl phosphoramide as a strong chiral Brønsted acid and its application to asymmetric Diels– Alder reaction. *J. Am. Chem. Soc.* **2006**, *128*, 9626-9627.

[9] Schreyer, L.; Properzi, R.; List, B. IDPi catalysis. *Angew. Chem., Int. Ed.* **2019**, *58*, 12761-12777.

[10] Betinol, I. O.; Lai, J.; Thakur, S.; Reid, J. P. A Data-Driven Workflow for Assessing and Predicting Generality in Asymmetric Catalysis. *J. Am. Chem. Soc.* **2023**, ASAP. *https://doi.org/10.1021/jacs.3c03989*.

[11] Reid, J.P.; Goodman, J.M. Goldilocks catalysts: computational insights into the role of the 3, 3′ substituents on the selectivity of BINOL-derived phosphoric acid catalysts. *J. Am. Chem. Soc.* **2016**, *138*, 7910-7917.

[12] Reid, J.P.; Goodman, J.M. Selecting chiral BINOL - derived phosphoric acid catalysts: general model to identify steric features essential for enantioselectivity. *Chem.-Eur. J.* **2017**, *23*, 14248-14260.

[13] Reid, J.P.; Ermanis, K.; Goodman, J.M. BINOPtimal: a web tool for optimal chiral phosphoric acid catalyst selection. *Chem. Commun.* **2019**, *55*, 1778-1781.

[14] (a) Kaib, P.S.; Schreyer, L.; Lee, S.; Properzi, R.; List, B. Extremely active organocatalysts enable a highly enantioselective addition of allyltrimethylsilane to aldehydes. *Angew. Chem., Int. Ed.* **2016**, 55, 13200-13203. (b) Gatzenmeier, T.; Turberg, M.; Yepes, D.; Xie, Y.; Neese, F.; Bistoni, G.; List, B. Scalable and highly diastereo-and enantioselective catalytic Diels–Alder reaction of α, β-unsaturated methyl esters. *J. Am. Chem. Soc.* **2018**, *140*, 12671-12676. (c) Lee, S.; Kaib, P.S.; List, B. Asymmetric catalysis via cyclic, aliphatic oxocarbenium ions. *J. Am. Chem. Soc.* **2017**, *139*, 2156-2159.

[15] (a) Bae, H.Y.; Höfler, D.; Kaib, P.S.; Kasaplar, P.; De, C.K.; Döhring, A.; Lee, S.; Kaupmees, K.; Leito, I.; List, B. Approaching sub-ppm-level asymmetric organocatalysis of a highly challenging and scalable carbon–carbon bond forming reaction. *Nature Chem* **2018**, *10*, 888-894. (b) Maji, R.; Ghosh, S.; Grossmann, O.; Zhang, P.; Leutzsch, M.; Tsuji, N.; List, B. A Catalytic Asymmetric Hydrolactonization. *J. Am. Chem. Soc.* **2023**, *145*, 8788–8793.

[16] Schwengers, S.A.; De, C.K.; Grossmann, O.; Grimm, J.A.; Sadlowski, N.R.; Gerosa, G.G.; List, B. Unified approach to imidodiphosphate-type Brønsted acids with tunable confinement and acidity. *J. Am. Chem. Soc.* **2021**, *143*, 14835-14844.

[17] Kaib, P.S.; Schreyer, L.; Lee, S.; Properzi, R.; List, B. Extremely active organocatalysts enable a highly enantioselective addition of allyltrimethylsilane to aldehydes. *Angew. Chem., Int. Ed.* **2016**, *55*, 13200-13203.

[18] Liu, L.; Kaib, P.S.; Tap, A.; List, B. A general catalytic asymmetric Prins cyclization. *J. Am. Chem. Soc.* **2016**, *138*, 10822-10825.
[19] Díaz-Oviedo, C.D.; Maji, R.; List, B. The catalytic asymmetric intermolecular Prins reaction. *J. Am. Chem. Soc.* **2021**, *143*, 20598-20604.
[20] Reddy, B.S.; Reddy, S.G.; Reddy, M.R.; Bhadra, M.P.; Sarma, A.V.S. Tandem Prins/pinacol reaction for the synthesis of oxaspiro [4.5] decan-1-one scaffolds. *Org. Biomol. Chem.* **2014**, *12*, 7257-7260.
[21] Chung, L.W.; Sameera, W.M.C.; Ramozzi, R.; Page, A.J.; Hatanaka, M.; Petrova, G.P.; Harris, T.V.; Li, X.; Ke, Z.; Liu, F.; Li, H.B. The ONIOM method and its applications. *Chem. Rev.* **2015**, *115*, 5678-5796.